Electronic Supplementary Material (ESI) for New Journal of Chemistry.

Investigation on $NiWO_4$/PANI Composite as Electrode Material for Energy Storage Devices

S. Rajkumar [a], S. Gowri [b], S. Dhineshkumar [a], J. Princy Merlin [a, *], A. Sathiyan [a, *]

[a] PG & Research Department of Chemistry, Bishop Heber College (Autonomous), Affiliated to Bharathidasan University Tiruchirappalli-620 017, Tamil Nadu, India.

[b] Department of Physics, Cauvery College for Women, Affiliated to Bharathidasan University, Tiruchirappalli-620 018, Tamil Nadu, India.

Corresponding Authors

Dr. J. Princy Merlin *E-mail: pmej_68@yahoo.co.in*

Dr. A. Sathiyan *E-mail: sathyanandraj@gmail.com*

1. Differentiating Capacitive Effect from CV analysis

A closer examination of the voltammetric scan rate dependence enables one to distinguish quantitatively the capacitive contribution to the current response. Using the concepts presented above, we can express the current response at a fixed potential as being the combination of two separate mechanisms, surface capacitive effects and diffusion-controlled insertion processes [1-5].

$$\mathbf{i\,(V)} = k_1 v + k_2 v^{1/2} \quad \textbf{……..(S1)}$$

For analytical purposes, we divide both sides of this equation with the square root of the scan rate, then:

$$\mathbf{i\,(V)} / v^{1/2} = k_1 v^{1/2} + k_2 \quad \textbf{……..(S2)}$$

In eqn. (S2), i(V) is the current at a given voltage, v is the scan rate, k_1 and k_2 are scan rate independent constants and k_1 v and k_2 $v^{1/2}$ correspond to the current contributions from the surface capacitive effects and the diffusion-controlled intercalation process, respectively. Then, the scan

rate dependence of the current according to eqn. (S2) was plotted and shown in Fig.S2. The linear behaviour enables us to determine k_1 and k_2 from the slope and the y-axis intercept of the straight line at each given voltage, respectively [2, 6].

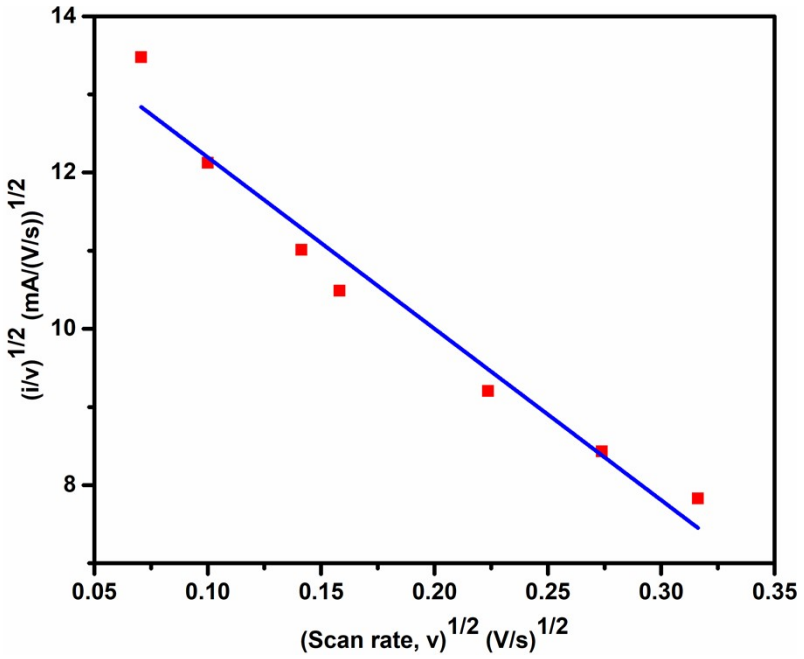

Fig. S1: Use of eqn. (2) to analyze the voltammetric sweep data for $NiWO_4$/PANI electrode at different scan rates varied from 5 to 100 mV s^{-1}

Another method was also developed to separate capacitive elements from insertion processes by Trasatti [2, 7]. The specific capacity (C_s) decreased as the scan rate increases and these data can be plotted versus an appropriate function of $v^{-1/2}$ or $v^{1/2}$ (Fig. S2), the scan rate, with the aim to extrapolate the values of C_s to v = 0 and v = ∞. If we allowed sufficient time for every reaction to take place, C_g at 0 mV s^{-1} will demonstrate the total capacitance (C_{tot}), while C_g at infinity will give us only the charge stored at the surface capacitance (C_{sur}). Then the capacitance related to the diffusion capacitance (C_{dif}) can be obtained from the difference between total and surface capacitance (C_{tot} - C_{sur}).

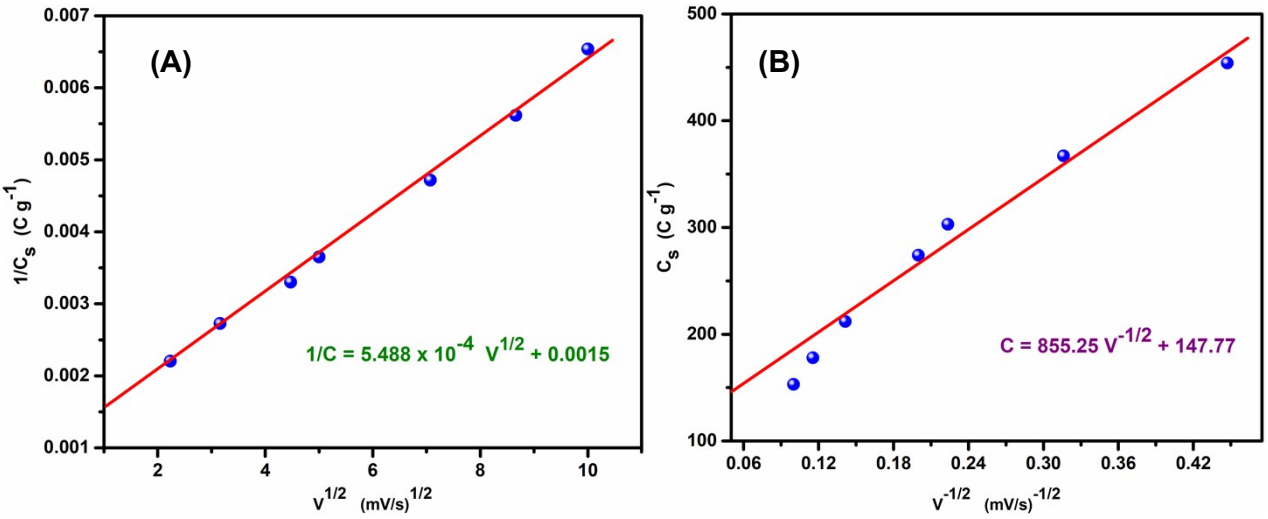

Fig.S2: A) Plot of reciprocal of Specific capacity (C_s^{-1}) vs. square root of scan rate ($v^{1/2}$) for $NiWO_4$/PANI Composite
B) Plot of Specific capacity (C_s) vs. reciprocal of square root of scan rate ($v^{-1/2}$) for $NiWO_4$/PANI Composite. The solid lines are linear fitting lines of data points

1.1 Evaluation of the percentage of capacity contribution from surface and diffusion-controlled processes in the total stored charge

The capacity contribution can be evaluated based on the following equations S3 & S4.

$$C_{sur}\,\% = \frac{C_{sur}}{C_T} \times 100\% \qquad \ldots\ldots\ldots\ldots\ldots\ldots (S3)$$

$$C_{dif}\,\% = \frac{C_{dif}}{C_T} \times 100\% \qquad \ldots\ldots\ldots\ldots\ldots\ldots (S4)$$

Where $C_{sur}\,\%$ and $C_{dif}\,\%$ stand for capacity percentage of surface and diffusion-controlled capacities.

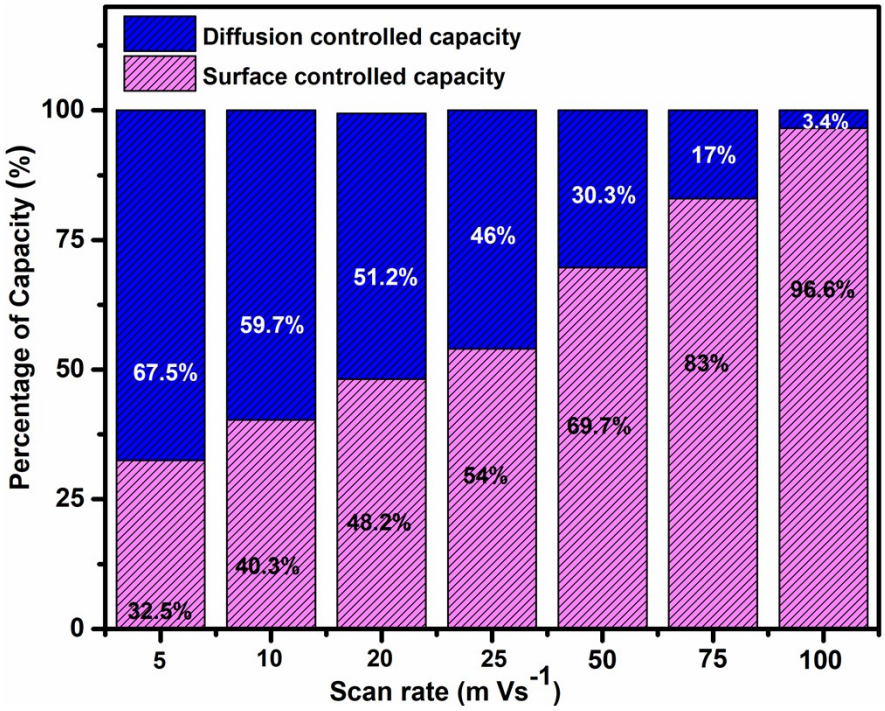

Fig. S3: Percentage of Capacity contribution evaluated for $NiWO_4$/PANI Composite at different scan rates (5 mVs^{-1} to 100 mVs^{-1})

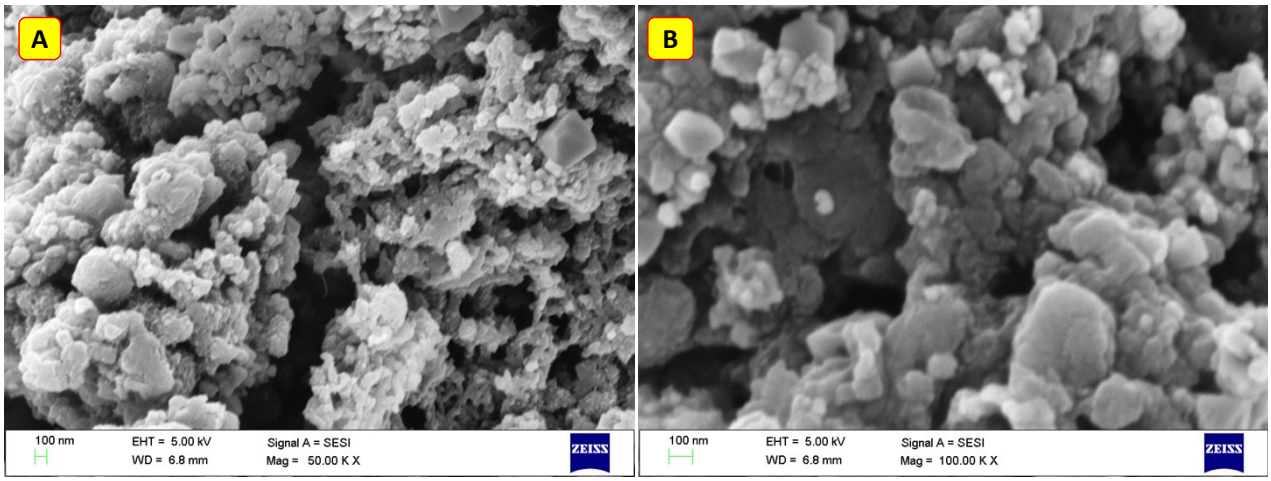

Fig. S4: FESEM Images of $NiWO_4$/PANI Composite before and after 5000 GCD cycles

References

[1] J. Wang, J. Polleux, J. Lim, B. Dunn, Pseudocapacitive contributions to electrochemical energy storage in TiO2 (anatase) nanoparticles, The Journal of Physical Chemistry C, 111 (2007) 14925-14931.

[2] J. Shao, X. Zhou, Q. Liu, R. Zou, W. Li, J. Yang, J. Hu, Mechanism analysis of the capacitance contributions and ultralong cycling-stability of the isomorphous MnO 2@ MnO 2 core/shell nanostructures for supercapacitors, Journal of Materials Chemistry A, 3 (2015) 6168-6176.

[3] T. Li, Z. Liu, L. Zhu, F. Dai, L. Hu, L. Zhang, Z. Wen, Y. Wu, Cr 2 O 3 nanoparticles: a fascinating electrode material combining both surface-controlled and diffusion-limited redox reactions for aqueous supercapacitors, Journal of Materials Science, 53 (2018) 16458-16465.

[4] Y.-S. Zhang, C. Lu, Y.-X. Hu, B.-M. Zhang, J. Li, C.-Y. Tian, D.-T. Zhang, L.-B. Kong, M.-C. Liu, Assemble from 0D to 3D: anchored 0D molybdenum carbide on 3D octahedral amorphous carbon with excellent capacitive properties, Journal of Materials Science, 55 (2020) 15562-15573.

[5] P. Pazhamalai, K. Krishnamoorthy, V.K. Mariappan, S.-J. Kim, Blue TiO2 nanosheets as a high-performance electrode material for supercapacitors, Journal of colloid and interface science, 536 (2019) 62-70.

[6] W. Yan, J.Y. Kim, W. Xing, K.C. Donavan, T. Ayvazian, R.M. Penner, Lithographically patterned gold/manganese dioxide core/shell nanowires for high capacity, high rate, and high cyclability hybrid electrical energy storage, Chemistry of Materials, 24 (2012) 2382-2390.

[7] S. Ardizzone, G. Fregonara, S. Trasatti, “Inner” and “outer” active surface of RuO2 electrodes, Electrochimica Acta, 35 (1990) 263-267.